

# Response characteristics of CO<sub>2</sub> gas sensors using KSmSi<sub>2</sub>O<sub>6</sub> as electrolyte and Li<sub>2</sub>CO<sub>3</sub>/K<sub>2</sub>CO<sub>3</sub> as sensing electrode

Susumu Nakayama (Department of Applied Chemistry and Biotechnology, National Institute of Technology (KOSEN), Niihama College, s.nakayama@niihama-nct.ac.jp, Japan)

## Abstract

Two types of solid-state electrochemical cells were designed and their CO<sub>2</sub> gas-sensing characteristics were compared. One was a heterojunction-type sensor, whereas the other was a conventional homojunction-type sensor. A potassium ionic conductor was used as the solid electrolyte and lithium carbonate (Li<sub>2</sub>CO<sub>3</sub>) or potassium carbonate (K<sub>2</sub>CO<sub>3</sub>) were used as the sensing electrodes. The electromotive force (EMF) of the cell, having Li<sub>2</sub>CO<sub>3</sub> as the electrode (heterojunction-type sensor), increased linearly with an increase in the partial pressure of CO<sub>2</sub> gas. Similar behavior was observed in the cell using the K<sub>2</sub>CO<sub>3</sub> electrode (homojunction-type sensor). The slopes of Nernst's equation suggest that the two-electron reduction associated with the carbon dioxide molecules occurs on the sensing electrode. The EMF of the heterojunction-type sensor showed excellent performance, and the 90% EMF response time of this sensor at 450 °C was only a few minutes on changing the carbon dioxide partial pressure.

## Key words

potassium samarium silicate, ceramics, ionic conductivity, lithium carbonate sensor, potassium carbonate sensor

## 1. Introduction

Commercially available solid electrolyte type and infrared absorption type sensors are typically used for carbon dioxide (CO<sub>2</sub>) detection. The solid electrolyte type CO<sub>2</sub> sensor is advantageous in terms of miniaturization and cost reduction. Alkali or alkaline earth metal ionic conductors are gaining attention as solid electrolytes for CO<sub>2</sub> gas sensors owing to their high conductivity in the temperature range where their carbonates can stably exist (Yamamoto et al., 2020 and Zhu et al., 2013). There are many types of CO<sub>2</sub> gas sensors, such as sensors composed of Mg<sub>1.15</sub>Zr<sub>4</sub>P<sub>5.7</sub>Si<sub>0.3</sub>O<sub>24</sub> as a solid electrolyte and Na<sub>2</sub>CO<sub>3</sub> or K<sub>2</sub>CO<sub>3</sub> as the sensing electrode; or a NASICON (Na Super Ionic CONductor, Na<sub>3</sub>Zr<sub>2</sub>Si<sub>2</sub>PO<sub>12</sub>) disc as the solid electrolyte, (Li-Ba)CO<sub>3</sub> as the sensing electrode, and (Na-Ti-O) as the reference electrode (Ikeda et al., 1995; Pasierb et al., 2003; 2004; Shqau et al., 2004). In the present work, two different types of CO<sub>2</sub> gas sensor devices were designed using alkali-metal rare earth silicates, KSmSi<sub>2</sub>O<sub>6</sub>, as solid electrolytes for CO<sub>2</sub> gas sensing over a wide temperature range of 300–600 °C (Aung et al., 2005; Nakayama et al., 1995; 1997; 1998). The ionic conductivity of KSmSi<sub>2</sub>O<sub>6</sub> ceramic is approximately two orders of magnitude lower than that of Nasicon ceramic—which is the most studied solid electrolyte for CO<sub>2</sub> sensors; however, it has good sinterability, can produce dense bodies, and has excellent gas shielding properties. Among large ion-sized potassium, rubidium, or cesium ionic conductive ceramics, the ionic conductivity of KSmSi<sub>2</sub>O<sub>6</sub> ceramic is extremely high. The ionic conductivity in the operating temperature range (300–600 °C) of solid electrolyte CO<sub>2</sub> sensors

is sufficient for CO<sub>2</sub> detection. First is a conventional homojunction-type sensor, in which KSmSi<sub>2</sub>O<sub>6</sub> is combined with potassium carbonate (K<sub>2</sub>CO<sub>3</sub>) as a sensing electrode. Second is a heterojunction-type sensor that uses lithium carbonate (Li<sub>2</sub>CO<sub>3</sub>) as the sensing electrode. By using potassium ion conductive KSmSi<sub>2</sub>O<sub>6</sub> ceramic, the difference in the ion size of the alkaline species of a sensing electrode can be increased. Furthermore, the response characteristics of the two devices as CO<sub>2</sub> gas sensors were compared.

## 2. Experimental procedure

To prepare the KSmSi<sub>2</sub>O<sub>6</sub> ceramics, K<sub>2</sub>CO<sub>3</sub>, Sm<sub>2</sub>O<sub>3</sub>, and SiO<sub>2</sub> were mixed in ethanol using a ball mill. The mixture was then dried and calcined in air for 2 h at 800 °C. The obtained powder was again ball-milled into a finer powder and dried. It was then converted into a disc by pressing at 100 MPa and sintering at 1050 °C for 2 h. The resulting microstructure was observed using scanning electron microscopy (Hitachi X-560). The diameter and thickness of the disc after sintering were 8 and 2 mm, respectively. The disc was baked at 800 °C after both sides were coated with a Pt paste. Electrical conductivities were measured with a multi-frequency LCR meter (HP 4192A) in the frequency range of 100 Hz to 10 MHz and temperature range of 300 to 600 °C. The CO<sub>2</sub> gas sensors were composed of the following solid-state cell:

- Heterojunction type  
(–) air, Pt | KSmSi<sub>2</sub>O<sub>6</sub> | Pt, Li<sub>2</sub>CO<sub>3</sub>, CO<sub>2</sub>, O<sub>2</sub> (+)
- Homojunction-type  
(–) air, Pt | KSmSi<sub>2</sub>O<sub>6</sub> | Pt, K<sub>2</sub>CO<sub>3</sub>, CO<sub>2</sub>, O<sub>2</sub> (+)

The hetero- and homojunction-type sensors use Li<sub>2</sub>CO<sub>3</sub> and K<sub>2</sub>CO<sub>3</sub> as the sensing electrodes, respectively. The sensor

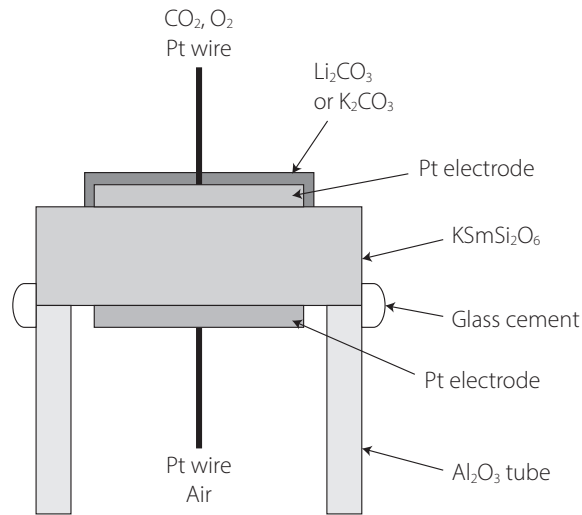


Figure 1: Schematic of CO<sub>2</sub> gas sensor

structure is shown in Figure 1. After both the sides (counter and sensing electrodes) of the KSmSi<sub>2</sub>O<sub>6</sub> disc were coated with Pt paste, the disc was baked at 800 °C for 30 min, and both sides were connected by Pt wires. Then, one of the Pt electrodes was immersed in an aqueous solution of M<sub>2</sub>CO<sub>3</sub> (M = Li or K) and dried to prepare the sensing electrode. This sensor system was fixed to one end of an alumina pipe with glass cement to shield the counter electrode from the CO<sub>2</sub> atmosphere. The standard CO<sub>2</sub> gases (1 × 10<sup>-5</sup> atm-, 1 × 10<sup>-4</sup> atm-, 1 × 10<sup>-3</sup> atm- and 1 × 10<sup>-2</sup> atm-CO<sub>2</sub>) diluted with syn-

thetic air were purchased from Sumitomo-seika Inc. Under these standard CO<sub>2</sub> atmospheres, the EMF was measured in the temperature range of 300-600 °C with a electrometer (Adventest TR8652).

### 3. Results and discussion

The KSmSi<sub>2</sub>O<sub>6</sub> ceramic disc formed after sintering was analyzed using scanning electron microscopy. The scanning electron microscopy images of (a) the fracture surface of the KSmSi<sub>2</sub>O<sub>6</sub> ceramic sintered at 1050 °C and (b) the surface

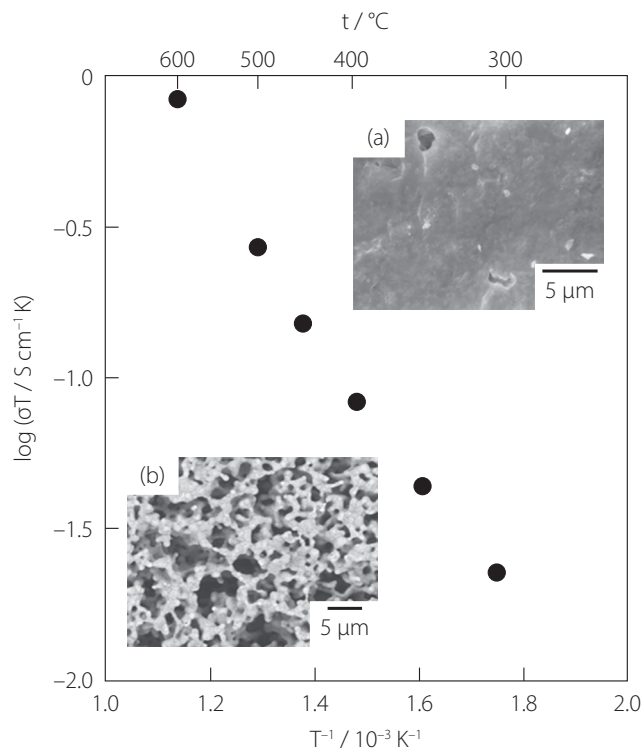


Figure 2: Arrhenius plot of log  $\sigma T$  vs.  $1/T$  for KSmSi<sub>2</sub>O<sub>6</sub> ceramic and the scanning electron microscopy images present in insets

Note: (a) the fracture surface of KSmSi<sub>2</sub>O<sub>6</sub> ceramic and (b) the surface of Pt electrode.

of the Pt electrode are shown in the inset of Figure 2. It is clear from the image that the sintering of KSmSi<sub>2</sub>O<sub>6</sub> ceramic progressed well, although some pores were observed. The Pt electrode exhibited uniform porosity over the surface. Further, the conductivity component (bulk and grain boundary components) of the KSmSi<sub>2</sub>O<sub>6</sub> ceramic was determined by performing complex-plane impedance analysis. The obtained conductivity components were parameterized based on the Arrhenius equation (Figure 2).

The dependence of EMF on the CO<sub>2</sub> partial pressure for the two types of CO<sub>2</sub> gas sensors at 450 °C is shown in Figure 3. The standard gases were passed through the sensing electrode side at the flow rate of 50 cm<sup>3</sup> · min<sup>-1</sup>. It was observed that the EMF of each sensor increased linearly with increasing log  $P_{CO_2}$ , and the dependence of the EMF on log  $P_{CO_2}$  obeys Nernst's equation. Meanwhile, the potential at the counter electrode, which is shielded from the detected CO<sub>2</sub> gas and exposed to an air atmosphere, was almost constant at a given temperature. This indicated that the observed EMF change was due to the potential change at the sensing electrode. Hence, the electron transfer number at the sensing electrode was estimated to be 2, calculated from the slope obtained from the linear regression analysis. This suggested that the CO<sub>2</sub> gas sensing in both types of sensors is based on a two-electron transfer reaction.

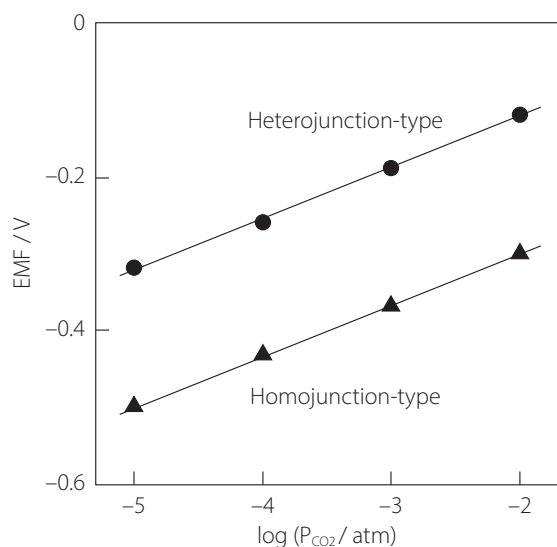


Figure 3: Dependence of sensor EMF on CO<sub>2</sub> partial pressure in air at 450 °C

Notes: Heterojunction-type sensor: Pt | KSmSi<sub>2</sub>O<sub>6</sub> | Pt, Li<sub>2</sub>CO<sub>3</sub>,  
Homojunction-type sensor: Pt | KSmSi<sub>2</sub>O<sub>6</sub> | Pt, K<sub>2</sub>CO<sub>3</sub>.

Further, the dependence of EMF on O<sub>2</sub> partial pressure (log  $P_{O_2}$ ) under  $1 \times 10^{-3}$  atm-CO<sub>2</sub> are shown in Figure 4. The EMF increases linearly with increasing log  $P_{O_2}$  and similar to the case of CO<sub>2</sub>, the dependence of EMF on log  $P_{O_2}$  obeys Nernst's equation. The electron transfer number estimated from the experimental slope is approximately 4, indicating

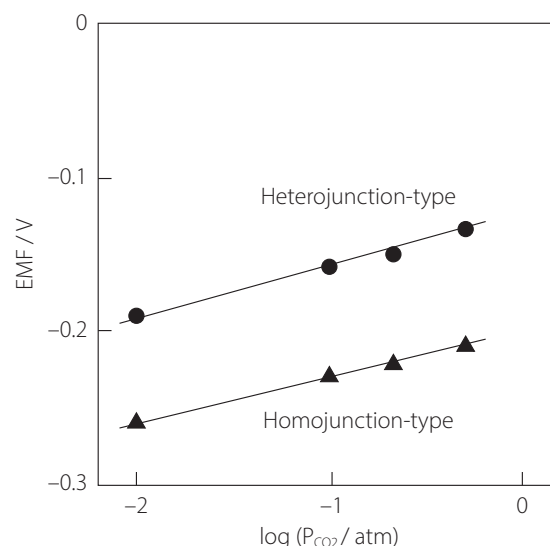


Figure 4: Dependence of sensor EMF on O<sub>2</sub> partial pressure in  $1 \times 10^{-3}$  atm-CO<sub>2</sub> pressure at 450 °C

that the four-electron reaction of O<sub>2</sub> is the method of detection at 450 °C.

Figure 5 shows the temperature dependence of EMF at  $1 \times 10^{-3}$  atm-CO<sub>2</sub> pressure. The EMF values decreased linearly with increasing temperature in the range of 350-550 °C. Furthermore, the temperature dependence of the potential at the detection electrode is linear in the range of 350-550 °C, indicating that the same electrode reaction occurs at the detection electrode in this range. Hence, the temperature dependence of the potential at the counter electrode is also expected to be linear.

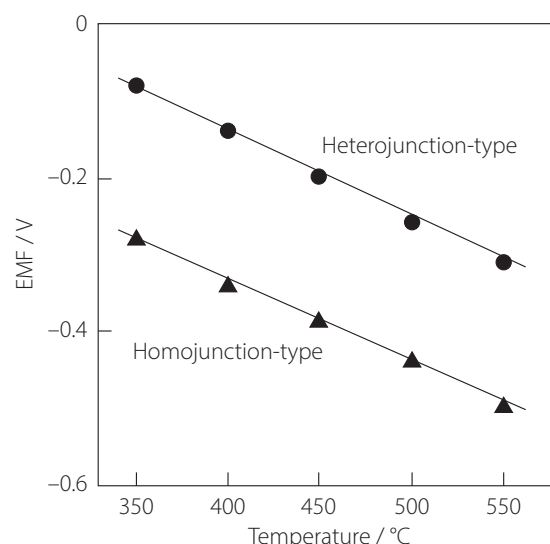


Figure 5: Temperature dependence of sensor EMF at  $1 \times 10^{-3}$  atm-CO<sub>2</sub> pressure in air

For approximately 1 month, the temperature was increased from room temperature to 450 °C every measurement day, and the EMF was measured to confirm the change in the

sensor response over time. In the heterojunction-type sensor, EMF increased by approximately 0.05 V until approximately 5 days, and then stabilized thereafter. In contrast, in the homojunction-type sensor, EMF decreased by approximately 0.03 V until approximately 5 days, and then stabilized thereafter. The tendency of the homojunction-type sensor was the same as that of the previously reported Pt | KSmSi<sub>3</sub>O<sub>8</sub> | Au, K<sub>2</sub>CO<sub>3</sub> sensor (Nakayama et al., 1997). In addition, it has been reported that the EMF and sensitivity of commercially available Nasicon electrolyte-based sensors are stable for a long period of 2 years (Kaneyasu et al., 1998).

Figure 6 shows the EMF response curves of the hetero- and homojunction-type sensors when the CO<sub>2</sub> gas concentration was changed in three steps from 1 × 10<sup>-4</sup> to 1 × 10<sup>-1</sup> atm. In the heterojunction-type sensor, the 90 % response times for an increase and decrease in CO<sub>2</sub> concentration were approximately 2 and 3 min, respectively. Meanwhile, in the homojunction-type sensor, the corresponding 90 % response times were approximately 5 and 10 min, respectively. Thus, the responses of both types of sensors were rapid, especially in the heterojunction-type sensors, and the reproducibility of the sensor EMF was also satisfactory. From these results, it can be assumed that the electrode reactions on the sensing electrode of both types of sensors are different, although two-electron reduction takes place. We assumed the following model for the solid electrolyte (KSmSi<sub>2</sub>O<sub>6</sub> ceramic)/sensing electrode interface grain boundaries of the solid electrolyte, which are invaded by carbonate as a sensing electrode mate-

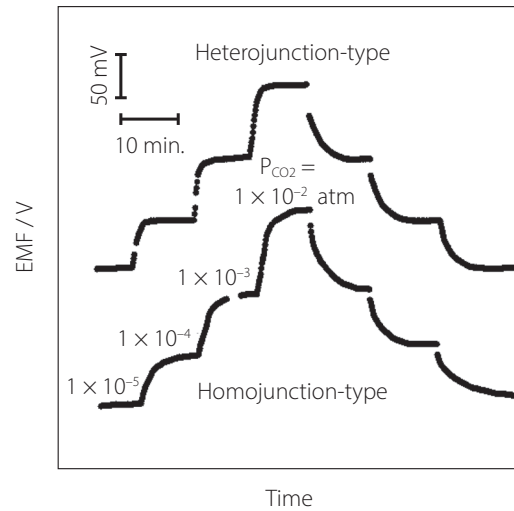


Figure 6: Response curves of sensor EMF in air at 450 °C

rial; the carbonate layer is very thin. It is considered that the carbonate present around the grain boundaries of the solid electrolyte is in redox equilibrium with the CO<sub>2</sub> gas captured on the sensing electrode, i.e., the solid electrolyte acts as a salt-bridge or supporting electrolyte. A schematic of the potential gradient at the interface between the solid electrolyte and sensing electrode is shown in Figure 7.  $E_1$  and  $E_2$  are the potentials corresponding to the change in the CO<sub>2</sub> gas concentration in the measurement atmosphere. The heterojunction-type sensor faces restricted ion diffusion and the layer of potential gradient is relatively narrow; meanwhile, in

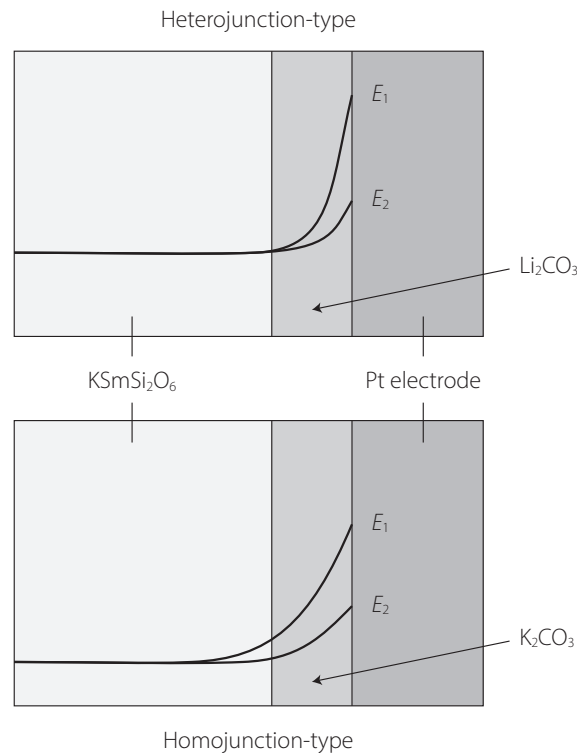


Figure 7: Schematic of the potential gradient at electrolyte/electrode interface

the homojunction-type sensor, ion diffusion is not restricted and the potential gradient occurs from the inside of the solid electrolyte. This is indicative of faster EMF response in the heterojunction-type sensor.

Considering the above results, the response mechanism of the CO<sub>2</sub> gas sensing was investigated. The counter electrodes of both types of sensors were always exposed to an atmosphere of 2.1×10<sup>-1</sup> atm oxygen partial pressure, and the electrode reaction can be expressed by the following equation:



The following reactions occur at the sensing electrode: in a heterojunction-type sensor,



In a homojunction-type sensor,



Here, these two reactions are represented by the following equation.



When Nernst's equation is applied to equations (1) and (2), the potential of the counter electrode,  $E_c$ , and the sensing electrode,  $E_s$ , are expressed by equations (3) and (4), respectively:

$$E_c = E'_c - (RT/2F) \ln(a_{K_2O} / a_{K^+}^2 \cdot (PO_2^I)^{1/2}) \quad (3)$$

$$E_s = E'_s - (RT/2F) \ln(a_{M_2CO_3} / a_{M^+}^2 \cdot (PO_2^{II})^{1/2} \cdot P_{CO_2}) \quad (4)$$

where  $E'$ ,  $R$ ,  $T$ ,  $F$ ,  $a_{K_2O}$ ,  $a_{K^+}$ ,  $a_{M_2CO_3}$ ,  $a_{M^+}$ ,  $PO_2$ , and  $P_{CO_2}$  are the standard electrode potential, gas constant, absolute temperature, Faraday constant, activities of K<sub>2</sub>O, K<sup>+</sup>, M<sub>2</sub>CO<sub>3</sub>, and M<sup>+</sup>, and the partial pressures of O<sub>2</sub> and CO<sub>2</sub>, respectively. As the  $E'_c$  and  $E'_s$  are constants, the EMF abbreviated as  $E$  is expressed as follows:

$$E = E_s - E_c \\ = E' - (RT/2F) \ln(a_{M_2CO_3} \cdot a_{K^+}^2 \cdot (PO_2^I)^{1/2} / a_{K_2O} \cdot a_{M^+}^2 \cdot P_{CO_2} \cdot (PO_2^{II})^{1/2}) \quad (5)$$

where  $E'$  is a constant. When the activities of M<sub>2</sub>CO<sub>3</sub>, M<sub>2</sub>O, Li<sup>+</sup>, K<sup>+</sup>, PO<sub>2</sub><sup>I</sup>, and PO<sub>2</sub><sup>II</sup> are kept constant, the CO<sub>2</sub> concentration can be calculated from the electromotive force  $E$ . Certainly, the results of the present CO<sub>2</sub> gas sensing can be reasonably explained by equation (5).

The ranges of electromotive force and operating temperature of the sensor reported in this study are almost the same

as those of commercially available Nasicon electrolyte-based sensors and other reported sensors. Therefore, it is considered that the same CO<sub>2</sub> detection circuit can be used.

#### 4. Conclusion

Two types of solid-state potentiometric CO<sub>2</sub> gas sensors consisting of a potassium ionic conductor, KSmSi<sub>2</sub>O<sub>6</sub> ceramic as a solid electrolyte, and metal carbonates (Li<sub>2</sub>CO<sub>3</sub> for heterojunction-type sensors and K<sub>2</sub>CO<sub>3</sub> for homojunction-type sensors) as a sensing electrode, were designed and their sensing properties were compared.

- The EMFs obeyed Nernst's equation for both hetero- and homojunction-type sensors.
- A two-electron transfer reaction associated with carbon dioxide molecules occurs on the sensing electrode. The carbonates Li<sub>2</sub>CO<sub>3</sub> and K<sub>2</sub>CO<sub>3</sub> used as sensing electrodes remain in redox equilibrium with the detected CO<sub>2</sub> gas.
- The 90 % EMF response times of both the hetero- and homojunction-type sensors was rapid; however, it was more pronounced in the former.

#### Acknowledgement

We would like to thank Editage (www.editage.com) for English language editing.

#### References

- Aung, Y. L., Nakayama, S., and Sakamoto, M. (2005). Electrical properties of MREGeO<sub>4</sub> (M=Li, Na, K; RE=rare earth) ceramics. *Journal of Materials Science*, Vol. 40, 129-133.
- Ikeda, S., Kondo, T., Kato, S., Ito, K., Nomura, K., and Fujita, Y. (1995). Carbon dioxide sensor using solid electrolytes with zirconium phosphate framework (2). Properties of the CO<sub>2</sub> gas sensor using Mg<sub>1.15</sub>Zr<sub>4</sub>P<sub>5.7</sub>Si<sub>0.3</sub>O<sub>24</sub> as electrolyte. *Solid State Ionics*, Vol. 79, 354-357.
- Kaneyasu, K., Otsuka, K., Setoguchi, Y., Nakahara, T., Sonoda, S., and Aso, I. (1998). A carbon dioxide gas sensor based on solid electrolyte for air quality control. *IEEE Transactions on Electrical and Electronic Engineering*, Vol. 118-E, No. 2, 199-127. (in Japanese)
- Nakayama, S. and Sadaoka, Y. (1995). Morphology and Ionic Conductivity of Potassium-Samarium-Silicates, K<sub>2</sub>O-Sm<sub>2</sub>O<sub>3</sub>-nSiO<sub>2</sub> (n=1-14). *Electrochimica Acta*, Vol. 40, 2541-2546.
- Nakayama, S., Kuwata, S., Sato, M., Sakamoto, M., and Sadaoka, Y. (1997). CO<sub>2</sub> gas sensor using the potassium ionic conductor K<sub>2</sub>O-Sm<sub>2</sub>O<sub>3</sub>-6SiO<sub>2</sub>. *Journal of the Ceramic Society of Japan*, Vol. 105, 255-257.
- Nakayama, S., Kuwata, S., Ichimori, T., Okazaki, M., Okamasa, M., Imai, S., Sakamoto, M., and Sadaoka, Y. (1998). Ionic conductivity of MAISi<sub>2</sub>O<sub>6</sub> (M = Li, Na, K, Rb and Cs) and its application as a potentiometric CO<sub>2</sub> gas sensor. *Journal of the Ceramic Society of Japan*, Vol. 106, 715-718.

- 
- Pasierb, P., Komornicki, S., Gajerski, R., Kozinski, S., and Rekas, M. (2003). The performance and long-time stability of potentiometric CO<sub>2</sub> gas sensors based on the (Li-Ba) CO<sub>3</sub>|NASICON|(Na-Ti-O) electrochemical cells. *Solid State Ionics*, Vol. 157, 357-363.
- Pasierb, P., Komornicki, S., Kozinski, S., Gajerski, R., and Rekas, M. (2004). Long-term stability of potentiometric CO<sub>2</sub> sensors based on Nasicon as a solid electrolyte. *Sensors and Actuators B: Chemical*, Vol. 101, 47-56.
- Shqau, K., Nafe, H., Aldinger, F., and Figueiredo, F. M. (2004). Determination of the p-electronic conduction parameter of NASICON by potentiometric measurements. *Electrochimica Acta*, Vol. 49, 2691-2696.
- Yamamoto, A., Shinkai, T., Loy, A. C. M., Mohamed, M., Baldovino, F. H. B., Yusup, S., Quitain, A. T., and Kida, T. (2020). Application of a solid electrolyte CO<sub>2</sub> sensor to the performance evaluation of CO<sub>2</sub> capture materials. *Sensors and Actuators B: Chemical*, Vol. 315, 128105.
- Zhu, Z., Thangadurai, V., and Weppner, W. (2013). Garnet-like solid state electrolyte Li<sub>6</sub>BaLa<sub>2</sub>Ta<sub>2</sub>O<sub>12</sub> based potentiometric CO<sub>2</sub> gas sensor. *Sensors and Actuators B: Chemical*, Vol. 176, 284-289.

(Received: March 24, 2022; Accepted: April 6, 2022)